Available online at www.springerlink.com

Acta Metall. Sin. (Engl. Lett.) Vol.26 No. 6 pp. 735—741 December 2013

ACTA
METALLURGICA SINICA
(ENGLISH LETTERS)

The Influence of Ultrasonic Frequency on the Properties of Ni-Co Coatings Prepared by Ultrasound-assisted Electrodeposition

Minqi SHENG[1,2)†], *Chenkai LV*[1)], *Lan HONG*[1)], *Mingwang SHAO*[2)], *Kang WAN*[1)] *and Fan LV*[1)]

1) School of Iron and Steel, Soochow University, Suzhou 215021, China

2) Institute of Functional Nano & Soft Materials (FUNSOM), Soochow University, Suzhou 215123, China

[Manuscript received 24 March 2013, in revised form 5 September 2013]

In this paper, Ni-Co coatings were electrodeposited onto carbon steel substrates with the aid of ultrasonic agitation. The coatings were analyzed by energy dispersive X-ray analysis (EDX), X-ray diffraction analysis (XRD) and scanning electron microscopy (SEM). The effects of the ultrasonic frequency on the roughness, hardness and corrosion resistance of the Ni-Co coatings were also investigated. The results indicated that the increase of the ultrasonic frequency from 20 to 120 kHz reduced the Ni content and the grain size of Ni-Co coatings. Moreover, the phase structure of the electrodeposited coatings was influenced by the ultrasonic frequency. Under 55 kHz ultrasonic agitation, the Ni-Co coating was single fcc phase and showed the finest roughness and the strongest corrosion resistance in 5 wt.% NaCl solution at the ambient temperature. Under ultrasonic agitation with frequency of 90 kHz, the coating was a mixture of fcc and hcp structure and showed the maximal hardness of about 420 HV. Therefore, ultrasonic agitation helped decrease the roughness, and enhance hardness and corrosion resistance of Ni-Co coatings.

KEY WORDS: Ni-Co alloys; Coatings; Electrodeposition; Ultrasound; Hardness; Corrosion

1. Introduction

Ni-Co alloy coatings have attracted widely attention due to its hardness and corrosion resistance as a replacement for hard chromium coating[1−4]. As the properties of Ni-Co coatings are seriously affected by their composition and structure, a reliable control of the composition and structure was an important issue for their wide applications. Many researchers investigated extensively the preparation of Ni-Co coating by direct current electrodeposition[5], pulse current electrodeposition[6] or pulse reverse current electrodeposition[7]. The composition and structure of Ni-Co coatings could be controlled by changing the electrodeposition parameters, such as overvoltage, current density, pulse parameters in pulsed electrodeposition[6−10]. Yet, more investigation was needed to obtain Ni-Co coatings with higher hardness and anti-corrosion.

In recent years, ultrasound-assisted electrodeposition applied to deposit various metals (or alloys) and composite coatings due to the advantages, such as increasing the deposition rate, decreasing the internal stress of the deposited coatings, and reducing additives in the plating bath[11−15]. Although there were many works on ultrasound-assisted electrodeposition[11−20], there was no report about the influence of ultrasonic frequency on the composition, structure and properties of Ni-Co coatings up to now.

In this study, the ultrasound-assisted electrodeposition was employed to deposit Ni-Co coatings. The influences of ultrasonic frequency on the composition, structure, roughness, hardness and corrosion resistance of the Ni-Co coatings were investigated. The results showed that the ultrasonic frequency (0–120 kHz) had significant impact on the characteristics

† Corresponding author. Ph.D.; Tel.: +86 18251186252; Fax: +86 512 67160032; E-mail address: smqtg@hotmail.com (Minqi SHENG)

DOI: 10.1007/s40195-013-0162-4

and properties of the obtained Ni-Co coatings.

2. Experimental

Carbon steel plates were used as substrates. The exposed area of these pretreated carbon steel substrates was equal to 1 cm^2 while the other surface areas were sealed with epoxy resin before the deposition. The electrodeposition was carried out in a conventional three-electrode cell connected with a Princeton VersaSTAT4 electrochemistry workstation. A platinum plate with an area of 2 cm^2 was used as the anode, and a saturated calomel electrode (SCE) was used as the reference electrode. Ultrasonic agitation was performed in an ultrasound-assisted electrodeposition setup with the output power of 100 W. The temperature of the water bath was controlled by a temperature controller. The detailed bath composition and experimental parameters are listed in Table 1 and 2.

Table 1 Bath compositions for Ni-Co alloy coatings deposition

Bath composition	Concentration (g/L)
$NiSO_4{\cdot}6H_2O$	110.0
$NiCl_2{\cdot}6H_2O$	6.0
$CoSO_4{\cdot}6H_2O$	55.0
H_3BO_3	12.5
$C_6H_8O_9$	5.6

Table 2 Experimental parameters for Ni-Co alloy coatings deposition

Parameter	Value
pH value	4.0
Temperature, T	40 °C
Current density, j	80 mA·cm^{-2}
Time, t	15 min
Ultrasonic frequency, f	0, 20, 55, 90 and 120 kHz

The phase structure, composition, and morphology of as-deposited coatings were investigated by X-ray diffraction spectrometer (D/max-2200V) with a CuK_α radiation, energy dispersive X-ray spectrometer (Oxford Instruments) and scanning electron microscopy (JEOL JSM-6700F).

The roughness of Ni-Co coatings was measured for 10 spots on each sample by a roughness meter (TR200). The Vickers hardness of Ni-Co coatings was measured using a microhardness tester (HXD-1000B) by loading a force of 0.245 N for 15 s, and the average of 10 hardness measurement results was taken as the hardness value. In order to investigate the corrosion resistance of Ni-Co coatings, the electrochemical behavior of the samples was analyzed by polarization plots and electrochemical impedance spectroscopy, using a Princeton VersaSTAT4 electrochemistry workstation. Polarization measurements were performed in 5 wt.% NaCl solution at the ambient temperature with a potential scan rate of 1 mV·s^{-1}. Electrochemical impedance spectroscopy tests were carried out potentiostatically at corrosion potential (E_{corr}), with the voltage perturbation amplitude of 10 mV in the frequency range from 10 kHz to 0.01 Hz.

3. Results and Discussion

3.1 Composition of Ni-Co coatings

Fig. 1 shows the EDX measured Ni contents of the Ni-Co coatings deposited under different frequencies ultrasonic. It is clearly observed that the Ni content in the coatings deposited under ultrasonic agitation is higher than that under silent condition (0 kHz), and the Ni content decreases with the ultrasonic frequencies increase from 20 kHz to 120 kHz.

During Ni-Co co-deposition process, the pH value at the cathode surface is found to rise due to H^+ ions consumption near the electrode and resulting in hydroxide ions increase[21–23]. The local increase of pH results in the formation of hydroxide precipitate of the low electrode potential metal Co and $CoOH^+$, followed by its adsorption onto the cathode surface[21–24]. This can be expressed as follows:

$$2H^+ + 2e^- \rightarrow H_2$$

$$2H_2O + 2e^- \rightarrow H_2 + 2OH^-$$

$$Co^{2+} + OH^- \rightarrow CoOH^+$$

$$CoOH^+ \rightarrow Co(OH)^+_{ads}$$

The adsorbed cobalt hydroxide ($Co(OH)^+_{ads}$) occupies the reaction sites, so that the deposition of the Ni which has high electrode potential metal is suppressed[21,24]. When applying ultrasonic agitation, the asymmetrical collapse of cavitation bubbles originated from the ultrasonic cavitation induces the formation of high velocity jets of liquid toward the cathode surface[18]. As a result, the desorption of $Co(OH)^+_{ads}$ on the cathode surface is enhanced by the liquid jets, and consequently more reaction sites are available for Ni deposition to enrich the Ni-Co coating with Ni.

It should be pointed out that with the increase in the ultrasonic frequency, the intensity of high velocity jets decreases since the ultrasonic cavitation decays[19]. Therefore, less $Co(OH)^+_{ads}$ is desorbed and there are fewer reaction sites for Ni deposition on the cathode surface when the ultrasonic frequency is high, leading to the low Ni content in Ni-Co coatings (shown in Fig. 1). These analyses confirm that the variation of the ultrasonic frequency can influence the electrodeposition process of Ni-Co coating.

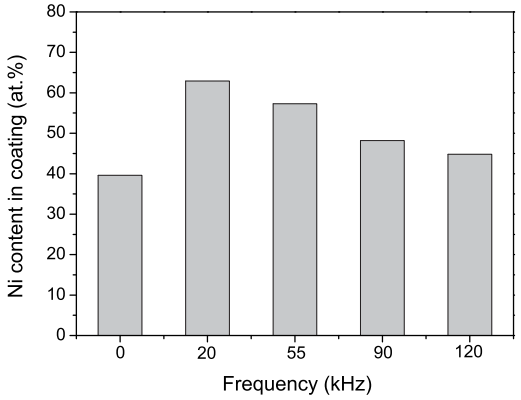

Fig. 1 The Ni contents of the Ni-Co coatings deposited under different frequencies ultrasonic

3.2 Phase structure and morphology of Ni-Co coatings

Fig. 2 shows the XRD patterns of the as-deposited coatings. The absence of Fe diffraction peak indicates that the carbon steel substrates are completely covered by the coatings. In XRD patterns, the fcc (α-Ni) contributes to (111), (200) and (220) planes while the hcp (ε-Co) contributes to (100), (002), (101) and (110) planes. Under 20 and 55 kHz ultrasonic agitation, no other diffraction peak is found except those peaks of fcc phase with a slight shift compared with those of pure Ni (JCPDS file No.04-0850). It is mainly because the Co atoms are incorporated into the crystalline lattice of Ni. Under other deposition conditions, the diffraction peaks of hcp phase reveal the formation of a mixed crystal structure. Tury *et al.*[25] pointed out that in this mixed crystal structure either a hexagonal Co cluster containing cubic structured Ni or a hexagonal Co cluster was built in the cubic structured Ni.

The grain size of Ni-Co coatings is determined using the Scherrer expression from XRD line broadening, as listed in Table 3. It is clearly showed that the introduction of ultrasonic agitation into the electrodeposition can refine the grain size. This is caused mainly by the following two reasons: (1) the high pressure acoustic steaming can interrupt the growth of grains; (2) the number of crystal nuclei on the cathode surface is increased under ultrasonic irradiation, because the instant local super cooling effect (caused by ultrasonic cavitation) decreases the radius of nucleation and leads to the increase of the nucleation rate.

From Table 3, it can also be observed that the grain size of the coatings decreases with the ultrasonic frequency in the range of 20 kHz to 120 kHz. The work of Coury *et al.*[26,27] and Compton *et al.*[28] have shown that the decrease in the intensity of ultrasonic cavitation leads to the increase in the thickness of diffusion layer, which finally gives an increasement in overpotential. It has been proved that a higher overpotential would boosts the nucleation rates and results in smaller nucleus radius[29]. Moreover, the intensity of ultrasonic cavitation decreases with the ultrasonic frequency increases[19]. Accordingly, the coatings deposited under higher frequency ultrasonic agitation posses finer grains.

Table 3 The grain sizes of Ni-Co coatings deposited under different frequencies ultrasonic

0 kHz	20 kHz	55 kHz	90 kHz	120 kHz
61.6 nm	39.3 nm	31.7 nm	25.2 nm	14.5 nm

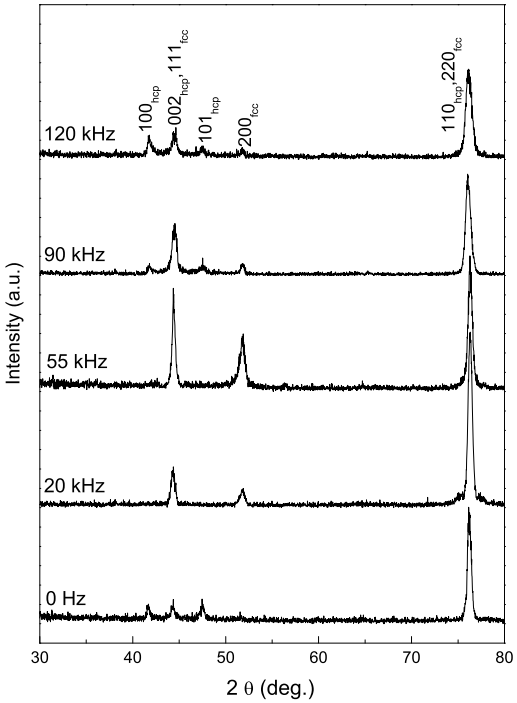

Fig. 2 XRD patterns of the Ni-Co coatings deposited under different frequencies ultrasonic

As shown in the SEM image (Fig. 3(a)), the as-deposited coating under silent condition exhibits a highly rough surface, which is quite different from those under ultrasonic agitation. In the case of silent electrodeposition, the coating surface is covered by large spherical clusters composing of random distributed dissimilar grains.

When applying 20 kHz ultrasonic agitation, the morphology of the Ni-Co coatings changes to regularly branched acicular structure as shown in Fig. 3(b). The acicular crystallites have an average length of 3–4 μm. By increasing the ultrasonic frequency to 55 kHz, the surface morphology as in Fig. 3(c) consists of pyramidal-shaped compact crystallites surrounded by tiny particles. The morphology of the Ni-Co coatings is composed of smaller spherical clusters when the ultrasonic frequency is increased further, as shown in Fig. 3(d) and (e).

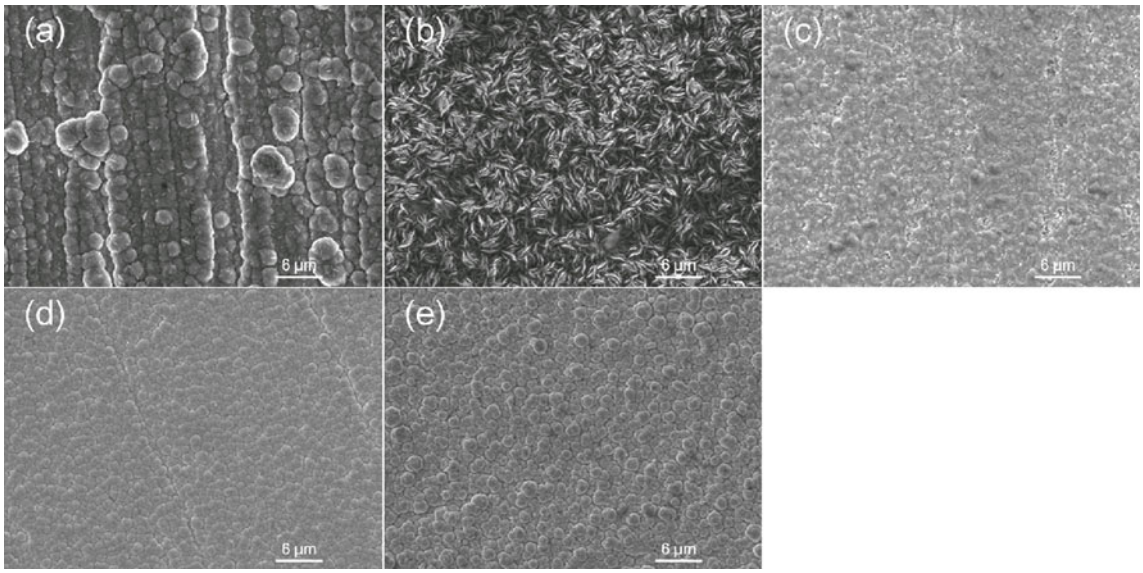

Fig. 3 Surface morphologies of the Ni-Co coatings deposited under different frequencies ultrasonic: (a) 0 kHz; (b) 20 kHz; (c) 55 kHz; (d) 90 kHz; (e) 120 kHz

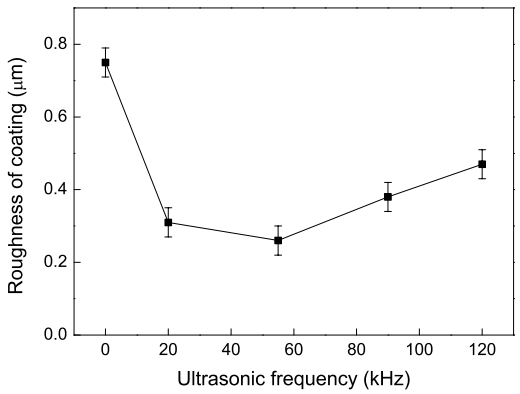

Fig. 4 The roughness of Ni-Co coatings deposited under different frequencies ultrasonic

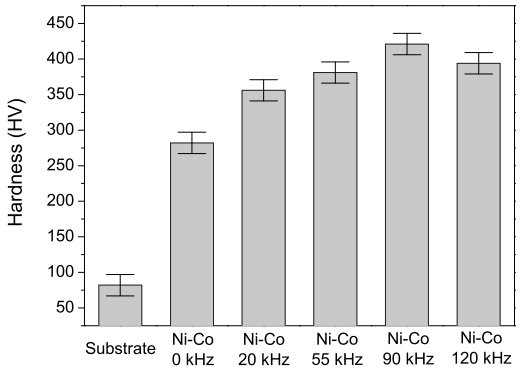

Fig. 5 The Vickers hardness of carbon steel substrate and Ni-Co coatings deposited under different frequencies ultrasonic

3.3 Evaluation of surface roughness

The calculated surface roughness parameters (R_a, arithmetical mean deviation of the assessed profile) are shown in Fig. 4. The roughness of the Ni-Co coatings deposited under ultrasonic agitation is finer than that under silent condition. A possible reason is that the amount of crystal nuclei on the carbon steel surface increases under ultrasonic agitation. The grain size becomes smaller when more nuclei are formed, which makes more even coating surface, as shown in Fig. 3 and Table 3.

3.4 Evaluation of hardness

The hardness results are shown in Fig. 5. All the Ni-Co coatings are harder than the carbon steel substrate. The hardness of the coatings increases with the increase of the ultrasonic frequency up to 90 kHz, and then decreases slightly as the ultrasonic frequency larger than 90 kHz. Under 90 kHz ultrasonic agitation, the hardness reached a maximum value of about 420 HV. The initial hardness increase (0–90 kHz) could be attributed to the grain size refinement effect, while the decrease of hardness at higher ultrasonic frequency (120 kHz) could be explained with the inverse Hall-Petch relation[30].

Fig. 6 shows the polarization plots of samples in 5 wt.% NaCl solution at ambient temperature. Table 4 lists the data for corrosion potential (E_{corr}), current density (i_{corr}), anodic/cathodic Tafel slope (b_a and b_c) and polarization resistance (R_p) obtained from the polarization plots. It can be clearly observed from Fig. 6 that the carbon steel substrate reacts drastically with the NaCl solution, while all the Ni-Co coatings have more positive corrosion potential, much lower corrosion current density and higher polarization resistance. In contrast with the blank carbon steel substrate and the coating deposited under silent condition, all the coatings deposited under ultrasonic agitation have more positive corrosion potential, lower

Table 4 Corrosion potential, current density, anodic/cathodic Tafel slope and polarization resistance obtained from the polarization plots as shown in Fig. 6

Sample	E_{corr} (V)	i_{corr} (μA·cm^{-2})	b_a (mV·dec^{-1})	b_c (mV·dec^{-1})	R_p (Ω·cm^{-2})
Substrate	−0.747	16.217	122.726	99.386	1.471×10^3
Ni-Co (0 kHz)	−0.658	6.124	104.637	101.413	3.652×10^3
Ni-Co (20 kHz)	−0.556	1.235	87.441	105.519	1.682×10^4
Ni-Co (55 kHz)	−0.478	0.778	84.353	98.173	2.532×10^4
Ni-Co (90 kHz)	−0.601	2.116	90.212	104.452	9.931×10^3
Ni-Co (120 kHz)	−0.628	5.848	101.457	97.821	4.195×10^3

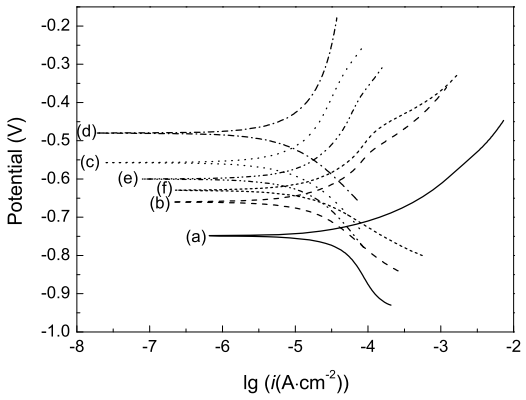

Fig. 6 Polarization plots of carbon steel substrate (a) and Ni-Co coatings prepared under different ultrasonic frequency of 0 kHz (b), 20 kHz (c), 55 kHz (d), 90 kHz (e) and 120 kHz (f)

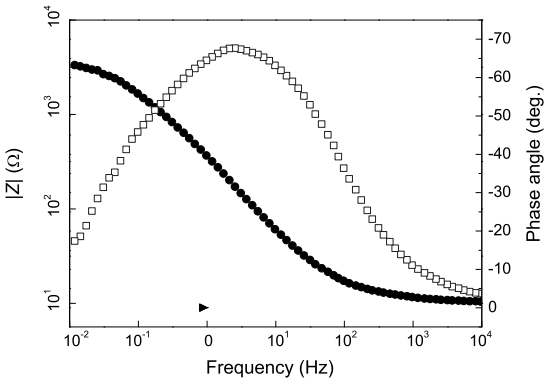

Fig. 7 Electrochemical impedance spectroscopy plots of carbon steel substrate

corrosion current density and higher polarization resistance. Among these coatings, the coating deposited under 55 kHz ultrasonic agitation shows the highest polarization resistance (R_p=2.532×10^4 Ω· cm^{-2}) and the lowest corrosion current density (i_{corr}=0.778 μA·cm^{-2}).

3.5 Evaluation of corrosion performance

Impedance plots (Bode plots) of the blank carbon steel substrate and the Ni-Co coatings are shown in Fig. 7 and Fig. 8, respectively. Bode plots of Frequency *vs.* phase angle exhibit a narrow peak, which indicates a single time constant for all the samples

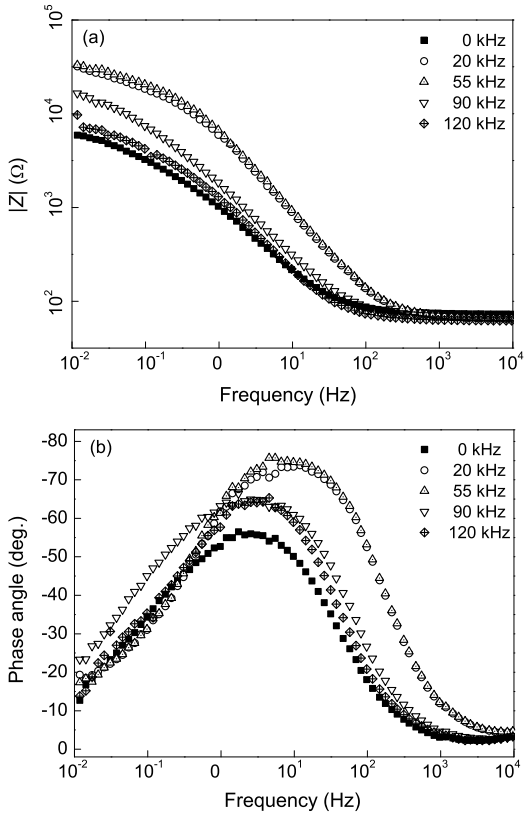

Fig. 8 Electrochemical impedance spectroscopy plots of Ni-Co coatings prepared under different ultrasonic frequency: (a) $|Z|$ *vs.* frequency; (b) phase angle *vs.* frequency

studied (Fig. 7 and Fig. 8(b)). The single peaks observed correspond to the metal/electrolyte interface. This behavior can be modeled as a parallel combination of a double electric layer capacitance and a charge transfer resistance.

An equivalent circuit is shown in Fig. 9. Here R_s is the solution resistance and Q_{dl} stands for the possibility of a non-ideal capacitance of a double electric layer (CPE, constant phase element) with various n_{dl}. The CPE represents a frequency dispersion of time constants originated from the local inhomogeneity or roughness or porosity of the surface[5]. R_{ct} is the charge transfer resistance of electrode reaction.

The calculated parameters are presented in Table 5. The R_{ct} values increase in the order: carbon steel substrate, Ni-Co (0 kHz), Ni-Co (120 kHz), Ni-Co (90 kHz), Ni-Co (20 kHz) and Ni-Co (55 kHz). The largest R_{ct} value is at 55 kHz for Ni-Co coat-

Table 5 Impedance parameters for carbon steel substrate and Ni-Co coatings

Sample	R_s (Ω)	Q_{dl} (μF·cm^{-2})	n_{dl}	R_{ct} (Ω·cm^{-2})
Substrate	6.547	38.957	0.89	4.124×10^3
Ni-Co (0 kHz)	5.904	66.789	0.79	7.686×10^3
Ni-Co (20 kHz)	8.326	45.568	0.86	3.488×10^4
Ni-Co (55 kHz)	6.896	37.456	0.87	4.321×10^4
Ni-Co (90 kHz)	4.987	51.321	0.82	1.723×10^4
Ni-Co (120 kHz)	7.132	43.905	0.81	8.926×10^3

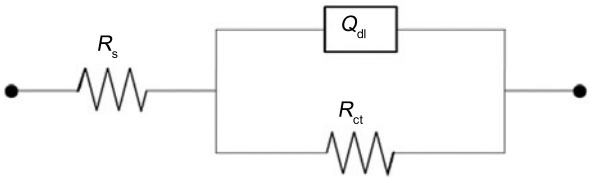

Fig. 9 Equivalent circuit for fitting the electrochemical impedance spectroscopy

ing indicates that the active area available for corrosive attack is less or alternatively the corrosion resistance is higher compared with others. The R_p values obtained from polarization studies has also exhibited similar pattern thereby affirming the above results.

From Table 5, it can be found that the Ni-Co (55 kHz) sample has the smallest Q_{dl} value, which implies that applying 55 kHz ultrasonic agitation can improve the surface morphology of the coating and decrease the surface defects. Further, n_{dl} values for carbon steel substrate, Ni-Co (20 kHz) and Ni-Co (55 kHz) lie in a narrow range of 0.86–0.89 demonstrate the low capacitive behavior of these samples. Whereas, the n_{dl} values for Ni-Co (0 kHz), Ni-Co (90 kHz) and Ni-Co (120 kHz) are less than 0.82, which suggests the much lower capacitive nature of these coatings. Bode plots (Fig. 7 and Fig. 8(b)) show that the phase angles of Ni-Co (0 kHz), Ni-Co (90 kHz) and Ni-Co (120 kHz) are distributed between 50° and 65°. As for carbon steel substrate, Ni-Co (20 kHz) and Ni-Co (55 kHz), the phase angles are within the range of 70°–75°, which also reveals better capacitive behaviors.

4. Conclusions

The results of the current study can be summarized as follows:

(1) The Ni-Co coatings produced by eletrodeposition method under ultrasonic agitation were uniform, compact and composed of fine grains.

(2)The ultrasonic frequency had a significant impact on the composition and grain size of the Ni-Co coatings. Both the Ni content and the grain size of Ni-Co coatings decreased with the ultrasonic frequency from 20 kHz to 120 kHz.

(3) When electrodeposition was conducted under a proper ultrasonic frequency, all the properties of Ni-Co coatings could be improved. The hardness reached a maximum value of about 420 HV at 90 kHz. Whereas, the coating produced at 55 kHz exhibited the strongest corrosion resistance.

Acknowledgements

This work was financially supported by the National Nature Science Fund of China (No. 51204115).

REFERENCES

[1] T. Osaka, M. Takai, K. Ohashi, M. Saito and K. Yamada, Nature **392** (1998) 796.
[2] T. Osaka, Electrochim. Acta. **44** (1999) 3855.
[3] K.Y. Sasaky and J.B. Talbot, J. Eletrochem. Soc. **147** (2000) 189.
[4] D. Golodnitsky, N.V. Gudin and G.A. Volyanuk, J. Eletrochem. Soc. **147** (2000) 4156.
[5] M. Srivastava, V.E. Selvi, V.K.W. Grips and K.S. Rajam, Surf. Coat. Technol. **201** (2006) 3051
[6] B. Tury, M.L. Varsányi and S. Roy, Appl. Surf. Sci. **253** (2007) 3103.
[7] L.M. Chang, H.F. Guo and M.Z. An, Mater. Lett. **62** (2008) 3313.
[8] C. Lupi, A. Dell'Era, M. Pasquali and P. Imperatori, Surf. Coat. Technol. **205** (2011) 5394.
[9] L. Tian, J. Xu and S. Xiao, Vacuum **86** (2011) 27.
[10] C.D. Gu, J.S. Lian and Z.H. Jiang, Adv. Eng. Mater. **8** (2006) 252.
[11] H.Y. Zhang and M.Z. An, J. Alloys Compd. **459** (2008) 548.
[12] R. Kas, F.S. Ertas and Ö. Birer, Appl. Surf. Sci. **259** (2012) 501.
[13] M. Kim, F. Sun, J. Lee, Y.K. Hyum and D. Lee, Surf. Coat. Technol. **205** (2010) 2362.
[14] M. Sheng, C. Wang, Q. Zhong, Y. Wei and Y. Wang, Ultrason. Sonochem. **17** (2010) 21.
[15] E.G. Lecina, I.G. Urrutia, J.A. Diez, J. Morgiel and P. Indyka, Surf. Coat. Technol. **206** (2012) 2998.
[16] F. Xia, M. Wu, F. Wang, Z. Jia and A. Wang, Curr. Appl. Phys. **9** (2009) 44.
[17] T. Ohsaka, M. Isaka, K. Hirano and T. Ohishi, Ultrason. Sonochem. **15** (2008) 283.
[18] B.G. Pollet, J.Y. Hihn and T.J. Mason, Electrochim. Acta. **53** (2008) 4248.
[19] G.O.H. Whillock and B.F. Harvey, Ultrason. Sonochem. **4** (1997) 33.
[20] Y. Niu, J. Wei, Y.Yang, J. Hu and Z. Yu, Surf. Coat. Technol. **210** (2012) 21.

[21] R. Oriňáková, A. Oriňák, G. Vering, I. Talian, R. M. Smith and H. F. Arlinghaus, Thin Solid Films **516** (2008) 3045.
[22] L. Wang, Y. Gao, Q. Xue, H. Liu and T. Xu, Appl. Surf. Sci. **242** (2005) 326.
[23] A. Bai and C. Hu, Electrochem. Acta. **47** (2002) 3447.
[24] C.K. Chung and W.T. Chang, Thin Solid Films **517** (2009) 4800.
[25] B. Tury, M.L. Varsányi and S. Roy, Surf. Coat. Technol. **200** (2006) 6713.
[26] R.S. Hagan and L.A. Coury, Anal. Chem. **66** (1994) 399.
[27] E.L. Cooper and L.A. Coury, J. Eletrochem. Soc. **145** (1998) 1994.
[28] R.G. Compton, J.C. Eklund, S.D. Page, G.H.W. Sanders and J. Booth, J. Phys. Chem. **98** (1994) 12410.
[29] Y. Li, H. Jiang, W. Huang and H. Tian, Appl. Surf. Sci. **254** (2008) 6865.
[30] Y. Li, H. Jiang, D. Wang and H. Ge, Surf. Coat. Technol. **202** (2008) 4952.